Optimal Channel Adaptation of Scalable Video over a Multi-Carrier Based Multi-Cell Environment

Jincheol Park, Hyungkeuk Lee, Sanghoon Lee, *Member, IEEE* and Alan C. Bovik, *Fellow, IEEE*

Abstract—To achieve seamless multimedia streaming services over wireless networks, it is important to overcome inter-cell interference (ICI), particularly, in cell border regions. In this regard scalable video coding (SVC) has been actively studied due to its advantage of channel adaptation. We explore an optimal solution for maximizing the expected visual entropy over an orthogonal frequency division multiplexing (OFDM) - based broadband network from the perspective of cross-layer optimization. An optimization problem is parameterized by a set of source and channel parameters that are acquired along the user location over a multi-cell environment. A sub-optimal solution is suggested using a greedy algorithm that allocates the radio resources to the scalable bitstreams as a function of their visual importance. The simulation results show that the greedy algorithm effectively resists ICI in the cell border region, while conventional non-scalable coding suffers severely because of ICI.

Index Terms—Cross-layer optimization, scalable video coding (SVC), human visual system (HVS), visual entropy, unequal error protection (UEP), inter-cell interference (ICI), OFDM-based System.

I. INTRODUCTION

As they migrate toward 4th generation (4G) systems, seamless multimedia services are expected to emerge using owing to the availability of wider bandwidths with greatly improved spectral efficiency. In order to improve the overall link capacity needed to accommodate such seamless services, standards such as the world inter-operability for microwave access (WiMax) and the 3rd Generation Partnership Project (3GPP) long term evolution (LTE) system employ frequency reuse factors (FRF) of 1, i.e., each cell utilizes an entire bandwidth without the use of band division among neighboring cells. However, full usage of the bandwidth significantly increases inter-cell interference (ICI), particularly at cell borders. Thus, system performance is degraded at cell boundaries so that seamlessness may not be guaranteed due to severe ICI. In

J. Park, H. Lee and S. Lee are with Wireless Network Laboratory, Department of Electrical and Electronics Engineering, The Yonsei University, Seoul 120-749, Korea, tel : 82-2-2123-2767, fax : 82-2-313-2879 (e-mail: dewofdawn@yonsei.ac.kr; punktank@yonsei.ac.kr; slee@yonsei.ac.kr).
A.C. Bovik is with the Laboratory for Image and Video Engineering (LIVE), Department of Electrical and Computer Engineering, The University of Texas, Austin, TX, USA 78712-1084 (e-mail:bovik@ece.utexas.edu).

an effort to ameliorate ICI, several ICI mitigation strategies have been discussed in [1]-[2]. Nevertheless, there exists a trade-off between gain in throughput and decrease in outage probability, so that such non-uniform channel quality over the cell coverage region is inevitable. To provide more consistent visual quality over abrupt wireless channel environments, cross-layer optimization has been introduced to more efficiently utilize source and channel resources. An overview of cross-layer design approaches was described in [3], where system performance was improved via information exchange across protocol layers or via cooperation of application layer with lower protocol layers. Meanwhile, scalable extension of the H.264/AVC standard has been finalized, including the network adaptive coding method. Scalable video coding (SVC) divides the video sequences into multiple layers: a base layer and several enhancement layers [4][5]. Since the base layer contains visually important data, it has been shown that unequal error protection (UEP) schemes using SVC can achieve better quality by more heavily protecting the base layer as compared to the enhancement layer [6]. In [7]-[8], several joint source channel coding and cross-layer design approaches were analyzed by utilizing UEP on the scalable bit-streams. However, even if a high potential to obtain a performance gain exists, most approaches rely on heuristic adaptive source-channel coding techniques. These have the following three major drawbacks:

1) Lack of quality criteria: From the perspective of source modeling, there is a lack of criteria for characterizing quality as perceived by the human visual system (HVS) although significant gains have recently been made in full-reference image quality [9]. Most optimization schemes seek to minimize distortion relative to rate-distortion or to maximize the peak signal-to-noise ratio (PSNR). However, since it is well known that the mean square error (MSE) and the PSNR correlate poorly with perceived quality, the measurement of the performance gain using traditional image quality criteria is suspect [10].

2) Coding redundancy of SVC: Although SVC presents definite advantages, coding efficiency is worse than for conventional non-scalable H.264/AVC. However, in [5], the performance of SVC is analyzed. It is found that an optimized encoder control can provide quality scalability at the cost of a bit rate increase of only 10% relative to non-scalable H.264/AVC coding.

3) Severe ICI near the cell border: In multi-cell environments, an FRF of 1 is considered to be a reasonable option, since the increase in total channel capacity is accompanied by ease of deployment. However, since full power is assigned to

each base station (BS) over the total bandwidth, severe ICI can occur, which in turn may lead to outages near the cell border [11].

Here we present a framework for cross-layer optimization that seeks to maximize visual quality considering the aforementioned issues. To unite the heterogeneous source and channel resources, visual entropy is employed in the objective function of the optimization problem. Visual entropy is a useful tool for quantifying the visual quality of the bit unit relative to visual perception [12]. In order to maximize the delivered visual entropy at the receiver, the cross-layer optimization scheme is performed between the application and medium access control / physical (MAC/PHY) layers in the protocol stack. The simulation results suggest a break-even point between the performance of scalable and non-scalable videos over a multi-cell environment. Although scalable video does not exhibit efficient performance in the inner region, it can effectively overcome ICI in cell border regions and provide acceptable quality at the receiver, while conventional non-scalable video suffers severely from ICI.

II. System Overview

Figure 1 shows the signal flow for the proposed cross-layer design. In the application layer of a multimedia source, the H.264/AVC based SVC makes it possible to generate scalable bitstreams as a function of the importance of each scalable bitstream. In the MAC/PHY layers of the BS and the MS, orthogonal frequency-division multiplexing (OFDM), which is generally adequate for multimedia transmission, is adopted. Owing to the characteristics of multicarrier modulation, it is possible to load scalable bitstreams into subcarriers dynamically. In order to make the channel adaptation scheme smoothly available, it is necessary to exchange information across the protocol stacks. The real-time transport protocol (RTP) and the real-time transport control protocol (RTCP) are used to deliver multimedia transmission and feedback in real-time video services [13].

A procedure for exchanging information between network nodes and across protocol stacks is depicted in Fig. 1. The channel condition is fed back from the PHY layer of the MS to the BS via a channel quality information (CQI) report in procedure (1). For example, in WiMax, the MS periodically reports CQI to the BS via the CQI channel (CQICH). At the same time, the PHY layer of the MS delivers the CQI report to the application layer via cross-layer management in procedure $(1)'$. In the BS, the MAC layer shares the CQI report from the PHY layer, for radio resource allocation in procedure (2). The application layer of the MS sends the RTCP feedback message (containing the CQI) to the multimedia source in procedure $(2)'$. It is possible to choose the application-specific message to be of the RTCP message type from among the five RTCP types. By receiving the CQI from the RTCP message, the multimedia source can estimate the expected visual entropy delivered over the wireless channel, so that a criterion can be provided to select a proper encoding method between the SVC and the non-SVC for a given channel status. Moreover, using the CQI, the multimedia source then estimates the target bit rate and performs rate control to select an optimal quantization step size. Although the transport control protocol (TCP) friendly rate control can be utilized to avoid congestion collapse, it cannot deal with effects caused by bit errors in the error prone wireless channel. Thus, the CQI is a crucial element of rate control. The encoded video data is organized into network abstraction layer (NAL) units that form the basic structure of an SVC bit stream. The multimedia source forwards the NAL units encapsulated in the RTP packet to the radio link buffer [6] at the BS in procedure (3). Here the MS plays the role of a media-aware network element (MANE) that can be aware of the information that is identified in the RTP and NAL unit header [14]. The encoding method is identified by the payload type (PT) in the RTP header, which indicates the media coding types for the RTP session. When SVC is determined to be the encoding method, the priority information for each layer is identified by the priority ID in the NAL unit header. Based on this information, the BS manages the radio link buffer to achieve channel adaptation, and transmits video data to the MS through the MAC/PHY layers. The radio link control (RLC) is a link-layer protocol that is responsible for error recovery and flow control.

III. Source Modeling for Quality Criterion

A. Rate and distortion Modelling

In [15], the classical rate distortion model is modified to yield rate $h(\Delta)$ and distortion $d(\Delta)$ models expressed in terms of the quantization step size Δ. In the H.264/AVC codec, the relationship between the quantization step size Δ and the QP q is expressed as $\Delta = 2^{q/6}$. The classical model is decomposed into two separate models as $h(\sigma^2, \Delta) = \frac{1}{2}\log_2\left(\frac{\epsilon^2 c \sigma^2}{\Delta^2}\right)$ and $d(\Delta) = \frac{\Delta^2}{c}$ where σ^2 denotes variance, c is 12 and ϵ^2 is about 1 assuming a uniform distribution, 1.4 for a Gaussian distribution, and 1.2 for a Laplacian distribution. The empirical rate of the original frame is defined by linearly scaling the classical rate model as $r(\sigma^2, \Delta) = \alpha h(\sigma^2, \Delta) + \beta$.

Suppose that Z is a random variable representing the sample points $h(\sigma^2, \Delta)$. The random variable R associated with $r(\sigma^2, \Delta)$ can then be expressed as $R = \alpha Z + \beta$, where α and β are constants. The expected value and variance of R are $E[R] = \alpha E[Z] + \beta$ and $VAR[R] = \alpha^2 VAR[Z]$. Therefore, $\alpha = \sqrt{VAR[R]/VAR[Z]}$ and $\beta = E[R] - \alpha E[Z]$.

By inserting σ^2 and Δ into the classical rate model $h(\sigma^2, \Delta)$, for each traffic measurement unit, the samples of Z can be obtained. Each macro block (MB) is used as a measurement unit. The samples of R are obtained from the SVC codec by counting the number of bits in each MB. The variance σ^2 is modified by ω_c. Thus the empirical rate model for each layer can be expressed as

$$r_b(\omega_c, \Delta_b) = \alpha_b h(\sigma^2(\omega_c), \Delta_b) + \beta_b \qquad (1)$$
$$r_e(\omega_c, \Delta_e) = \alpha_e h(\sigma^2(\omega_c), \Delta_e) + \beta_e$$

where r_b (r_e) is the empirical rate of the base layer (enhancement layer), $\omega_c = 2\pi f_c$ (f_c is the cutoff frequency), Δ_b (Δ_e) is the quantization step size of the base layer (enhancement layer), and α_b and β_b (α_e and β_e) are the base layer (enhancement layer) constants, respectively.
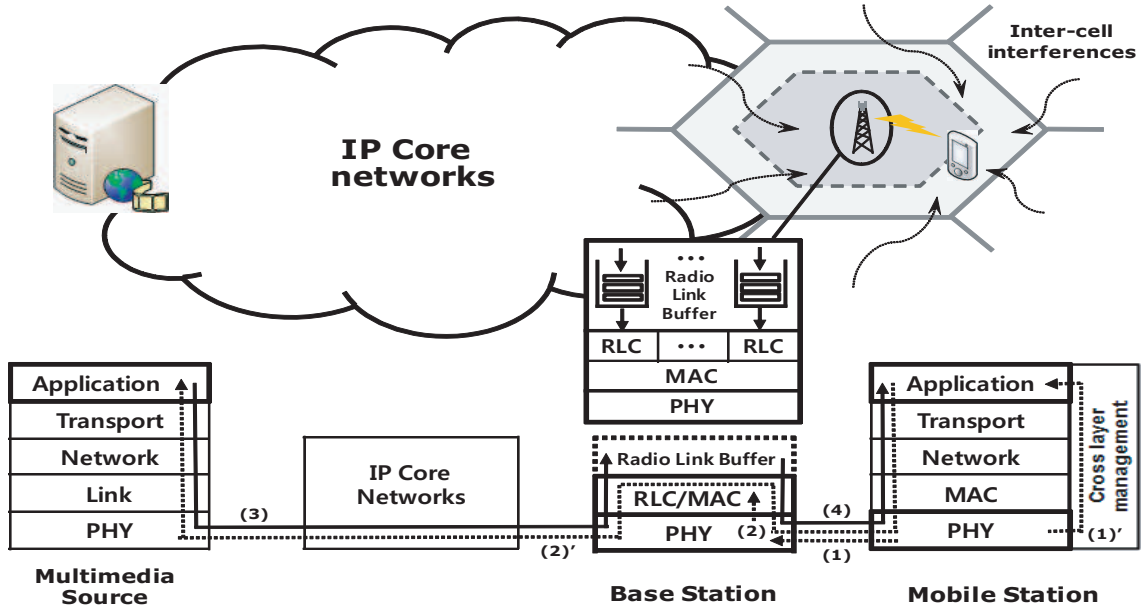
Fig. 1. Signal flows though network nodes and protocol stacks for the cross-layer design

B. Visual entropy and distortion

Many approaches to video compression and communication have sought to incorporate the CSF [16]-[19]. We utilize the CSF model developed in [16], owing to its relevance and simplicity, to construct visual weights in the discrete cosine transform (DCT)-domain, which is divided into two layers. In [16], the contrast threshold model was given by $CT(f, e_c) = CT_0 \exp\left(\lambda f \frac{e_c + e_2}{e_2}\right)$. Parameter values that fit human experimental data were introduced by [18]. As there we use $\lambda = 0.106$, $e_2 = 2.3$, and $CT_0 = 1/64$ [18]. The contrast sensitivity is taken to be the inverse of the contrast threshold as $CS(f, e_c) = 1/CT(f, e_c)$.

The visual angle between the fovea and a point on the retina with respect to the nodal point of the optics in the human eye is eccentricity. The eccentricity of each block is zero under the assumption that all regions are uniformly focused by the human eye. Then the CSF is written by $CS(f_1, f_2) = \frac{1}{CT_0} \exp\left(-\lambda\kappa\sqrt{f_1^2 + f_2^2}\right)$ where f_1 and f_2 are vertical and horizontal DCT frequencies and κ is a conversion constant (from DCT frequency to cycle/degree) [19]. When a frame is divided into two layers, the frequency range is split into $0 \sim f_c$ and $f_c \sim f_{max}$. To represent the visual weight of each layer, the expectation of the CSF is calculated as a function of frequency. We model the probability density function (PDF) of the DCT coefficients using an exponential form as $p(f_1, f_2) = \mu \exp\left(-\nu\sqrt{f_1^2 + f_2^2}\right)$.

Since the DC component is an average value, μ is the average value of the block coefficients. ν is a decay factor determined in order that the integral of PDF is unity. Using the CSF and the PDF, the expectation of the CSF (i.e. the visual weight) over the frequency domain is calculated as

$$\phi_{max} = \int_0^{f_{max}} \int_0^{f_{max}} p(f_1, f_2) \, CS(f_1, f_2) \, df_1 df_2$$

$$= \int_0^{f_{max}} \int_0^{f_{max}} A \, \exp(-B\sqrt{f_1^2 + f_2^2}) \, df_1 df_2$$

$$= \int_0^{\frac{\pi}{2}} \int_0^{f_{max}} A \, \exp(-Br) \, r dr d\theta$$

$$= \frac{A\pi}{2}\left(\frac{1}{B^2} - \left(\frac{f_{max}}{B} + \frac{1}{B^2}\right)e^{-Bf_{max}}\right) \quad (2)$$

where $A = \frac{\mu}{CT_0}$ and $B = \lambda\kappa + \nu$. A change of variables from Cartesian to polar coordinate is made to rewrite the integral. Although it is somewhat awkward to use the discrete variables f_1 and f_2 as variables of integration, we treat them as continuous variables for convenience of expression. Using ϕ_{max}, the normalized weight of each layer is given by

$$\phi_b(f_c) = \frac{\int_0^{f_c} \int_0^{f_c} p(f_1, f_2) \, CS(f_1, f_2) \, df_1 df_2}{\phi_{max}}$$

$$= \frac{\frac{A\pi}{2}\left(\frac{1}{B^2} - \left(\frac{f_c}{B} + \frac{1}{B^2}\right)e^{-Bf_c}\right)}{\phi_{max}}, \quad (3)$$

for the base layer, and

$$\phi_e(f_c) = \frac{\int_{f_c}^{f_{max}} \int_{f_c}^{f_{max}} p(f_1, f_2) \, CS(f_1, f_2) \, df_1 df_2}{\phi_{max}}$$

$$= \frac{\frac{A\pi}{2}\left(\left(\frac{f_c}{B} + \frac{1}{B^2}\right)e^{-Bf_c} - \left(\frac{f_{max}}{B} + \frac{1}{B^2}\right)e^{-Bf_{max}}\right)}{\phi_{max}}, \quad (4)$$

for the enhancement layer. The visual entropy is again defined as the expected number of bits required to visually perceive a macroblock (MB). Multiplying the empirical rate model of each layer (1) by the visual weight of the base layer ϕ_b and the enhancement layer ϕ_e, the visual entropy is defined as

$$h_b^w(\omega_c, \Delta_b) = \phi_b(f_c) \cdot r_b(\omega_c, \Delta_b)$$
$$h_e^w(\omega_c, \Delta_e) = \phi_e(f_c) \cdot r_e(\omega_c, \Delta_e) \quad (5)$$

for the base layer h_b^w and enhancement layers h_e^w, respectively. In addition, the visual distortion is similarly defined by

applying the visual weight to the classical distortion function, $d(\Delta)$, for the base layer d_b and the enhancement layer d_e:

$$
\begin{aligned}
d_b^w(\omega_c, \Delta_b) &= \phi_b(f_c) \cdot d_b(\Delta_b) \\
d_e^w(\omega_c, \Delta_e) &= \phi_e(f_c) \cdot d_e(\Delta_e)
\end{aligned}
\tag{6}
$$

for the base layer d_b^w and enhancement layer d_e^w, respectively.

IV. ICI ON THE OFDM BASED SYSTEM

In OFDM downlink transmission, the degree of ICI depends on the relative position and shadowing factors from surrounding BSs. Due to increases in multimedia service rates over the internet, more consistent visual quality is expected. Therefore, effective strategies are needed for providing more reliable high quality visual services over the entire cell coverage. We develop a fundamental cross-layer optimization approach, where the bandwidth allocated to each user is divided into two parts. We present the development for the case of two scalable layers, although it is extensible. In the general case of more layers than two, the bandwidth may be further sub-divided. One part of the bandwidth is assigned to the base layer, while the other part is assigned to the enhancement layers. When monitoring channel quality over the cell, the bandwidth of each layer is adapted to effectively deliver visual information by controlling the channel bit error rate (BER). To measure system performance, a multi-carrier system is analyzed over a multi-cell environment with an FRF of 1. An E_b/N_o formula is then derived in terms of bandwidth, path loss, the user bit rate and the allocated power. Using this formula, the BER is obtained at each position. BW_T is the total bandwidth of the system (Hz), BW_s is the bandwidth of a subcarrier (Hz), and BW_b and BW_e are the bandwidths allocated to the base layer and enhancement layers, respectively. Also, N_{sc}^T is the total number of sub-carriers, and N_{sc}^b and N_{sc}^e are the number of sub-carriers allocated to the base and enhancement layers, respectively. For brevity, the superscript or subscript 'l' indicates "of the lth layer" throughout the paper. In an OFDM based system, the bandwidth is given by $BW_l = (N_{sc}^l + 1) \cdot BW_s/2$ and $N_{sc}^l \leq N_{sc}^T$. The spectral efficiency is improved by overlapping the sidebands of the subcarriers, and by arranging the subcarriers to preserve orthgonality [20].
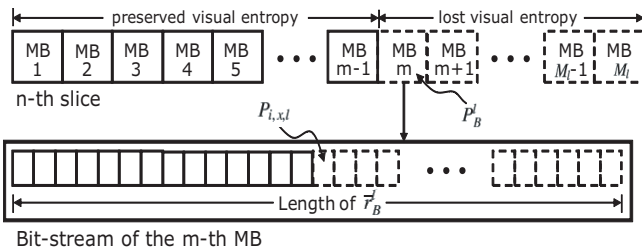
Fig. 2. The delivered and corrupted MBs when a transmission error occurs at the mth MB

Let an MS be located in position x of the ith BS (i.e., the home BS). Then, the path loss between the MS of the ith BS and an adjacent BS (here, the jth BS) is given by $L_{(i,x:j)} = r_{(i,x:j)}^{-p} 10^{\xi_{(i,x:j)}/10} = r_{(i,x:j)}^{-p} \chi_{(i,x:j)}$ where p is

a path-loss exponent (typically three to four), $r_{(i,x:j)}$ is the distance between x in the ith BS and the jth BS, $\xi_{(i,x:j)}$ is a Gaussian distributed random variable with zero mean and standard deviation representing shadowing, and $\chi_{(i,x:j)}$ is a lognormally distributed random variable. Typically, the standard deviation of ξ is in the range of 6-10 dB for signals from adjacent BSs and 2-2.5 dB for signals from the home BS [11][20]. Here, it is assumed that p=4. In the multi-carrier system, a hexagonal cellular pattern is assumed and a number of neighbor cells (N_{oc}=6) is assumed in the 1st tiers for calculation of the ICI.

Therefore, the ICI (I_{oc}) and the intra cell interference (I_{sc}) with respect to the ith home cell (here i= 0) are given by $I_{oc} = \sum_{j=1}^{N_{oc}} S \cdot L_{(i,x:j)}$ and $I_{sc} = \theta \cdot S(1 - \varepsilon_{i,x}) \cdot L_{(i,x:i)}$ where S is the total power of each BS, $\varepsilon_{i,x}$ is the normalized power of the MS located at position x in the ith BS, and θ is an orthogonality parameter.

In general, the signal to interference plus noise ratio (SINR) of the system at position x in the ith cell over the cellular system is given by $SINR_{i,x} = L_{(i,x:i)} \cdot S \cdot \varepsilon_{i,x}/(I_{oc} + I_{sc} + N_0 BW_T)$ where N_0 is the power spectral density of additive white Gaussian noise (AWGN). Therefore, if $I_{oc}+I_{sc} \gg N_0 BW_T$, then the SINR formula is $SINR_{i,x} =$

$$
L_{(i,x:i)} \cdot S \cdot \varepsilon_{i,x} / \left(\sum_{j=1}^{N_{oc}} S \cdot L_{(i,x:j)} + \theta \cdot S(1 - \varepsilon_{i,x}) \cdot L_{(i,x:i)} \right).
$$

The formula $(E_b/N_0)_{i,x,l}$ for the lth layer at position x in the ith cell is obtained by

$$
\left(\frac{E_b}{N_0} \right)_{i,x,l} = \frac{L_{(i,x:i)} \cdot S \cdot \varepsilon_{i,x} \cdot \frac{BW_l}{R_b^l}}{\sum_{j=1}^{N_{oc}} S \cdot L_{(i,x:j)} + \theta \cdot S(1 - \varepsilon_{i,x}) \cdot L_{(i,x:i)}}
\tag{7}
$$

where BW_l is the bandwidth and R_b^l is the user bit rate.

Using this result, the relation between the instantaneous BER and E_b/N_0 with the 4-QAM modulation for a Rayleigh fading channel is given by $P_{i,x,l} = Q \left(\sqrt{2|H|^2 \left(\frac{E_b}{N_0} \right)_{i,x,l}} \right)$ where the channel H is a circularly symmetric complex Gaussian random variable with mean 0 and variance 1. In the sequel, the BER will be utilized to obtain the probability that a MB contains bit errors in a video frame being transmitted over the network.

V. OPTIMIZATION OF EXPECTED VISUAL ENTROPY

A. Expected Visual Entropy

When the video data is transmitted over a noisy/fading channel, distortion is caused not only by quantization errors, but also by bit errors. The H.264/AVC codec uses entropy coding, so a bit error in the coded bit-stream is propagated to the end of the data due to the loss of synchronization. A synchronization unit consists of a slice, so the corrupted synchronization can be refreshed with the start of new slice. In our analysis, it is assumed that one bit error has influence from the block that contains an erroneous bit to the end of the slice.

In Fig. 2, the mth MB is corrupted due to a bit error. In such a case, the rest of the MBs to the end of slice are assumed to be lost, regardless of how many erroneous bits occur in subsequent MBs. In the following we derive the expected visual entropy for a given BER, where the unit of video data is taken to be the MB. Optimization of the expected visual entropy can then be formulated using several constraints.

Let P_B^l be the probability that a bit error occurs in a MB when the number of bits of the MB is given to $\bar{r}_B^l$. Suppose that the MS is located at a position "x" of the ith BS. Then, the BER is given by $P_{i,x,l}$. Using $P_{i,x,l}$, P_B^l can be obtained by $P_B^l = \sum_{i=1}^{\bar{r}_B^l} (1 - P_{i,x,l})^{i-1} \, P_{i,x,l}$.

Since all bit information following the first bit error is regarded as corrupted, all MBs following the mth MB containing the first bit error in the slice are treated as lost. Using our definition of visual entropy (5), the expected visual entropy in a frame can be written

$$\overline{h_l^w} = \sum_{n=1}^{N_l} \sum_{m=2}^{M_l} \sum_{k=1}^{m-1} h_{n,k}^{w,l}(\omega_c^l, \Delta_l)(1 - P_B^l)^{m-1} P_B^l$$
$$+ \sum_{n=1}^{N_l} \sum_{k=1}^{M_l} h_{n,k}^{w,l}(\omega_c^l, \Delta_l)(1 - P_B^l)^{M_l} \qquad (8)$$

where N_l is the number of slices in the lth layer and M_l is the number of MBs in a slice of the lth layer. The visual entropy of the lth layer in (5) is divided into elements $h_{n,k}^{w,l}$ indexed by slice n and by MB k. The former term is the expected visual entropy when a first bit error occurs at the mth MB, and the latter term is the expected visual entropy when no bit errors occur.

B. Optimization problem

The expected visual entropy can be represented by an objective function of a cross-layer optimization problem, parameterized by ω_c^l, q_l, N_{sc}^l, and R_b^l as

$$\max_{\omega_c^l, q_l, N_{sc}^l, R_b^l} \quad \sum_{l=0}^{L-1} \overline{h_l^w}(\omega_c^l, q_l, N_{sc}^l, R_b^l) \qquad (9)$$

$$\text{subject to} \quad \sum_{l=0}^{L-1} \frac{(N_{sc}^l + 1)BW_s}{2} \leq BW_T, \; R_b^l \geq 0$$

$$0 \leq \omega_c^l \leq \frac{1}{2}\pi, \; 1 \leq q_l \leq q_{max}$$

where L is the number of layers. Here $l = 0$ denotes a base layer and $l > 0$ denotes one or several enhancement layers. The number of sub-carriers is restricted by the bandwidth of a subcarrier and by the total bandwidth. The maximum QP, q_{max}, can take one of 52 values according to the H.264/AVC standard.

The problem posed above is computationally intractable due to the Q-function contained in the BER of the expected visual entropy. Thus, a direct approach to solving it does not yield a good algorithm. Therefore, we seek a close approximation to the optimal expected visual entropy, wherein the optimization problem is decomposed into distinct optimal rate control and
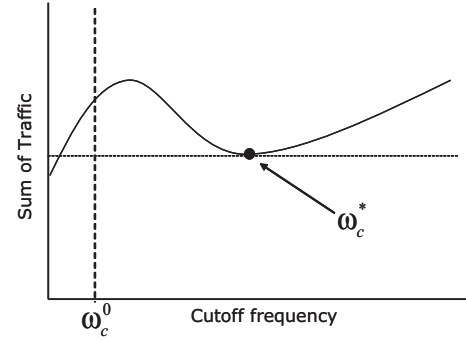
Fig. 3. Optimal cutoff frequency minimizing the sum of traffic

wireless channel adaptation problems. However, the simultaneous solution of these closely related problems requires a cooperative exchange of information. On the source side, for a given the available bit rate from the wireless channel the visually optimal bit rate is allocated by the Lagrangian method to each layer, as described in detail in Section V-C. On the channel side, for given priority information from the source side, we propose a greedy algorithm wherein the radio resources are preferentially allocated to the base layer, then the remainders are allocated to the enhancement layer in the manner of best effort, as described in detail in Section V-D. To avoid confusion, the notation is listed in Table I. The following is the overall framework for cross-layer optimization: **The first layer ($l=0$) is the base layer, while subsequent layers ($1 \leq l \leq L-1$) are enhancement layers.**

Step 1. CQI feedback: The MS feeds back CQI information to the multimedia source and to the BS

Step 2. Optimal rate control: For the multimedia source, find w_c^{l*} for which the sum of traffic generated by the base and enhancement layers is minimized, as shown in Fig. 3, but to make the scalable video meaningful, $w_c^{l*} \geq w_c^0$. At a given instant, fixing w_c^{l*}, find q_l^* using the optimal rate control where R_b^* is estimated from the reported CQI.

Step 3. Radio resource allocation: Given w_c^{l*} and q_l^* in step 2, determine R_b^l and N_{sc}^l. After sub-carrier allocation for the base layer is guaranteed, the remaining sub-carriers ($N_{sc}^T - N_{sc}^l$) are allocated to the subsequent enhancement layers

In Fig. 10, it is shown that the expected visual entropy delivered to the MSs decreases with the normalized distance due to ICI. Because of the coding efficiency, the expected visual entropy of non-scalable video is better than that of scalable video, when the channel state is reliable. However, if the channel becomes unreliable due to ICI, there exists a break-even point at which scalable video is better. The reason is the following. When a bit error occurs in transmission, the non-scalable video loses all visual entropy from the distorted points onward through following bits. However, in the case of scalable video, the base layer is guaranteed to be preserved. Thus, an opportunistic switching scheme can be developed using the break-even point in Fig. 10.

	Notation	Description
source side	ω_c^{l*}	Optimal cutoff frequency that minimizes the sum of the generated traffic of lth and $(l+1)^{th}$ layer.
	q_l^*	Optimal QP of the lth layer minimizing the visual distortion given the attainable user bit rate.
	$\widetilde{r}_l(\omega_c^l, q)$	Generated traffic per second in a frame of the lth layer, parameterized by cutoff frequency and QP.
	ω_c^0	Minimal cutoff frequency that is meaningful.
channel side	R_b^*	Maximal user bit rate, using total number of sub-carriers and satisfying the target BER.
	R_b^{l*}	User bit rate assigned for the lth layer.
	N_{sc}^T	Total number of remaining sub-carriers.
	N_{sc}^{l*}	Optimal number of sub-carriers for l^{th} layer to support the user bit rate.
	P^t	Target BER.
	$P_{i,x}(N_{sc}, R_b)$	BER parameterized by N_{sc} and R_b at a position x in the ith cell.
	$N_{sc}^{tmp1}, N_{sc}^{tmp2}$	Temporary variables for the number of sub-carriers

C. Visually optimal rate control

A rate control algorithm dynamically adjusts the QP to achieve a target bit rate. It allocates a budget of bits to divided groups in the video sequence. Here we deploy a frame level rate control algorithm using the Lagrangian method to allocate a visually optimal bit rate to each layer. This process is conducted in Step 2 of the cross-layer optimization framework. After determining the quantization step size Δ, the QP is calculated using the relation $\Delta = 2^{q/6}$. The rate control process consists of the following two major components.

1) Target bit rate estimation: The target bit rate $\overline{R}$ should be obtained for the current video frame of each layer in prior to calculating the optimal QP. A fluid flow traffic model can be used to compute the target bit rate, as in [21]. This approach considers the buffer status and the available bit rate, which can be estimated from the CQI. Assuming that the target bit rate mainly depends on the available bit rate, the former is a function of the latter. Then, we take $\overline{R} = R(R_b^*)$, where $R(\cdot)$ is the target bit rate estimation function derived from the fluid flow traffic model in [21].

2) Lagrangian method for optimal QP: Using the empirical rate $r(\sigma^2, \Delta)$, the target bit rate should be appropriately distributed to each layer by determining the quantization step sizes to minimize distortion. Here the Lagrangian method is used to minimize the visual distortion (6) using the bit rate constraint $\overline{R}$ and (1):

$$L(\Delta_k, \gamma) = \sum_{l=0}^{L-1} \sum_{m=0}^{M_l N_l - 1} d_l^w(\omega_c^{l*}, \Delta_l)$$
$$+ \gamma \left(\sum_{l=0}^{L-1} \sum_{m=0}^{M_l N_l - 1} r_l(\omega_c^{l*}, \Delta_l) - \overline{R} \right) \quad (10)$$

$$\approx \sum_{l=0}^{L-1} M_l N_l \phi_l \frac{\Delta_l^2}{c}$$
$$+ \gamma \left(\sum_{l=0}^{L-1} M_l N_l \left(\frac{\alpha_l}{2} \log_2 \left(\frac{\epsilon^2 c \overline{\sigma}_l^2}{\Delta_l^2} \right) + \beta_l \right) - \overline{R} \right) \quad (11)$$

where $\overline{\sigma}_l^2 = \frac{1}{M_l N_l} \sum_{m=0}^{M_l N_l - 1} \sigma_m^2(\omega_c^{l*})$ and γ is the Lagrange multiplier. In this optimization problem, the visual distortion serves as a utility function.

Differentiating it with respect to Δ_l and γ, the following Karush-Khun-Tucker (KKT) condition is obtained:

$$2M_l N_l \phi_l \frac{\Delta_l}{c} - \frac{\gamma M_l N_l \alpha_l}{\Delta_l \ln 2} = 0, \quad (12)$$
$$\gamma \left(\sum_{l=0}^{L-1} M_l N_l \left(\frac{\alpha_l}{2} \log_2 \left(\frac{\epsilon^2 c \overline{\sigma}_l^2}{\Delta_l^2} \right) + \beta_l \right) - \overline{R} \right) = 0, \quad (13)$$
$$\gamma \geq 0. \quad (14)$$

From (12), the optimal quantization step size for the lth layer Δ_l^* is obtained as $\Delta_l^* = \sqrt{\frac{\alpha_l \gamma c}{2 \phi_l \ln 2}}$. Inserting Δ_l^* into the complementary slackness condition (CSC) (13) and arranging it with respect to γ, the optimal Lagrange multiplier γ^* is obtained as $\gamma^* = 2^{\Pi}$ where

$$\Pi = \frac{\sum_{l=0}^{L-1} M_l N_l \left(\frac{\alpha_l}{2} \log_2 \left(\frac{2\epsilon^2 \phi_l \overline{\sigma}_l^2 \ln 2}{\alpha_l} \right) + \beta_l \right) - \overline{R}}{\sum_{l=0}^{L-1} \frac{M_l N_l \alpha_l}{2}}. \quad (15)$$

The empirical rate model(1) of each layer is used here to determine the optimal QP for rate control. However, to obtain samples of Z and R, a specific QP should be determined first. This is similar to the chicken-and-egg dilemma complicates rate control of H.264/AVC [21]. In [21], the dilemma is solved by predicting information, which is used in the rate distortion model, from the previous frame. Similarly, we can solve the dilemma by predicting R and Z from the previous frame.

D. Radio resource allocation

In OFDM based systems, channel estimation is critical to achieve performance enhancement. Most OFDM techniques use a pilot signal to measure the channel state. Using the pilot, the available bit rate can be estimated, and the estimate fed back to the multimedia source to achieve rate control. Although optimal rate control is achieved, wireless channel adaptation using priority information forwarded from the multimedia source is essential in a mobile network. This is true since, the closer the mobile node is to the cell boundary, the more susceptible the wireless channel condition is to ICI.

The computed visual weight of the base layer will be much larger than that of the enhancement layer in most cases. Therefore, the greedy scheme is proposed to allocate the sub-carriers of the OFDM-based system to the base layer in advance, with the remainder being allocated to the enhancement layers:

A greedy algorithm for radio resource allocation

for each layer l = 0 : L-1, **do**

$\quad R_b^{l*} = \widetilde{r}_l(\omega_c^{l*}, q^*)$

$\quad N_{sc}^{tmp1} = \arg\min_{0 \leq N_{sc} \leq N_{sc}^T} \left| P_{i,x}(N_{sc}, R_b^{l*}) - P^t \right|$

$\quad N_{sc}^{tmp2} = N_{sc}^T - N_{sc}^{tmp1}$

$\quad$**if** $N_{sc}^{tmp2} \geq 0$, **do**

$\qquad N_{sc}^{l*} = N_{sc}^{tmp1}, \ N_{sc}^T = N_{sc}^{tmp2}$

$\quad$**end if**

$\quad$**else if** $N_{sc}^T > 0$, **do**

$\qquad N_{sc}^{l*} = N_{sc}^T, \ N_{sc}^T = 0$

$\quad$**end else if**

$\quad$**else**, **do**

$\qquad N_{sc}^{l*} = 0, \ R_b^{l*} = 0$

$\quad$**end else**

end for

Fig. 4. Switching the encoding mode as a function of expected visual entropy comparison over a cell

E. Opportunistic switching of encoding mode

Figure 4 depicts the criterion for opportunistic encoding when switching the coding mode over a cell. The break-even point of the expected visual entropy is used as a reference point, to determine which encoding method is proper for a given channel state. The numbers '1', '2' and '3' indicate distinct switching as a function of the difference of the expected visual entropies between SVC and non-SVC. In region 1, $\overline{H}_S \leq \eta \overline{H}_N$, so the proper encoding method is non-SVC, where η is an adjustment parameter $(0 < \eta < 1)$, $\overline{H}_N$ is the expected visual entropy of non-SVC and $\overline{H}_S$ is the expected visual entropy of SVC. In region 3, $\overline{H}_N \leq \overline{H}_S$, so the proper encoding method is SVC. Region 2, where $\eta \overline{H}_N < \overline{H}_S < \overline{H}_N$, is an intermediate interval whose range is determined by η. In this interval, the difference of the expected visual entropy is not so large, and approaches a cross-point. Meanwhile, near the break-even point, the BER may be larger than the target BER owing to channel fluctuation, so that severe distortion may occur using non-SVC. Conversely, since the channel adaptation of SVC can overcome severe distortion from bit errors, using SVC prior to the break-even point in the region 2 is a more reliable choice. As can be seen in Fig. 4, the greater the distance from the BS, the wider the cell area. Let δ be the radius of the cell and ρ be the normalized distance of the break-even point. The area of the inner and outer regions are $\pi(\rho\delta)^2$ and $\pi(1-\rho^2)\delta^2$. If $\rho = 0.7$, the area of the inner region is almost the same that of the outer region, so the opportunistic switching method becomes useful.

VI. SIMULATION RESULTS

In our simulations, we utilized the empirical traffic model in (1) to measure the performance of our methods. The CIF sequences 'Akiyo' and 'Coastguard' were the test videos. Figure 4 and Fig. 5 compare the traffic for the empirical model and for the real encoded data, for each layer (1). In Fig. 5, the 1st sequence of 'Akiyo' was used with $q = 10$ and
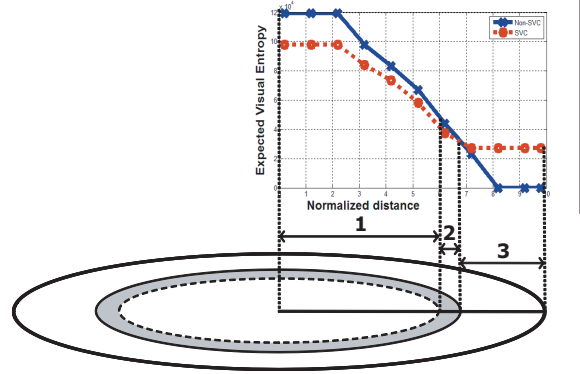
$w_c = 0.16\pi$, which optimally minimizes the traffic sum. In Fig. 6, the 11th frame of 'Coastguard' was used with $q = 10$ and $w_c = 0.16\pi$ which is also the optimal choice of w_c. The modeling parameters α and β are obtained from (4) and (5). For the base layer (enhancement layer) of the 1st 'Akiyo' sequence, the values obtained are $\alpha = 93.34$ and $\beta = -18.27$ ($\alpha = 39.82$ and $\beta = 65.94$). For the base layer (enhancement layer) of the 11th 'Coastguard' sequence, the values obtained are $\alpha = 124.64$ and $\beta = -96.51$ ($\alpha = 84.08$ and $\beta = -14.44$). It may be seen that the statistical behavior of the simulated traffic traces the real traffic relatively well, thus validating the empirical model relative to real traffic.

Figure 7 compares the average visual distortion of the proposed visually optimal rate control scheme with the encoder control used in JSVM [22], given a target bit rate. In JSVM the QP for the enhancement layer is set equal to the QP for the base layer plus 4 [22]. However it is not optimal relative to visual distortion as shown in (7). JSVM strictly allocates bit rate by lowering the QP of the base layer by 4. However, it does improve performance when it flexibly allocates bit rates to each layer using perceptual principles.
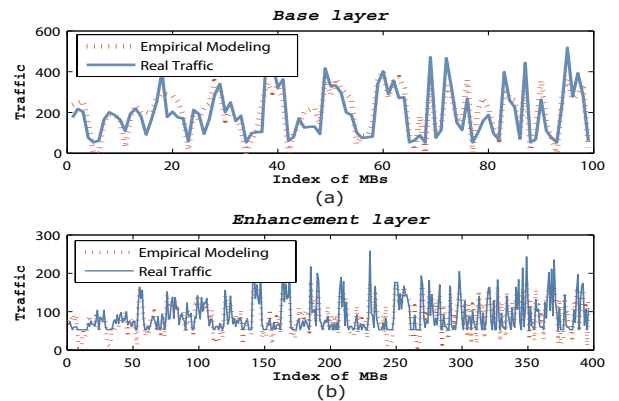
Fig. 5. Comparison of traffic between the empirical model and the real encoded traffic for base layer (a) and enhancement layer (b) of the 1st sequence of 'Akiyo'

In order to find an optimal cutoff frequency, the total traffic volume is measured as a function of cutoff frequency. The optimal cutoff frequency is determined when the total traffic
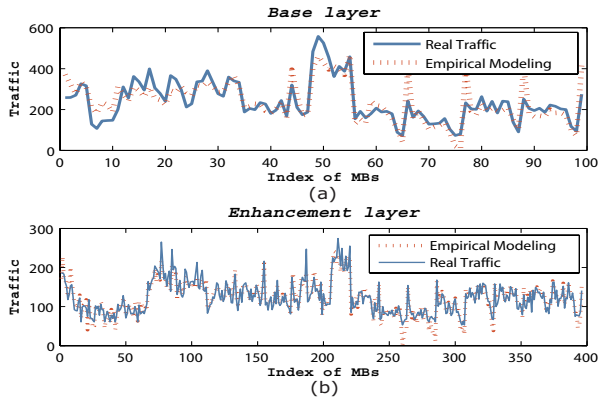
Fig. 6. Comparison of traffic between the empirical model and the real encoded traffic for base layer (a) and enhancement layer (b) of the 11th sequence of 'Coastguard'
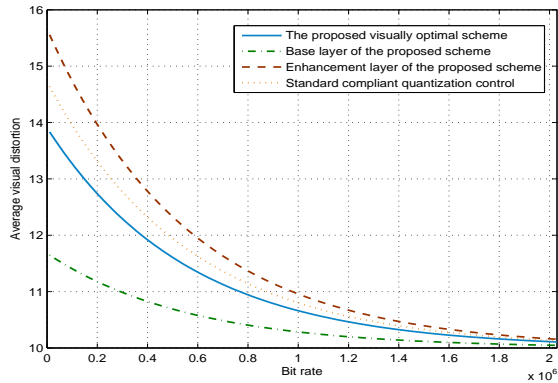
Fig. 7. Average visual distortion as a function of target bit rate

is at a minimum. Figure 8 shows the total traffic obtained by taking the sum of the two layers of traffic as a function of the cutoff frequency. Note that the traffic volume exhibits non-linear variation as a function of cutoff frequency for a given QP. Although the cutoff frequency changes the traffic volume, it does not directly induce distortion as quantization distortion does. Thus the cutoff frequency yielding the minimum sum of traffics is the optimal cutoff frequency. Using Step 2 of the optimal algorithm, an optimal cutoff frequency and an adequate QP can be determined.

To simulate the channel side, the parameter set in Table II is used. Figure 9 shows the ratio E_b/N_0 of the system model described in Section IV as a function of the normalized

TABLE II
THE SIMULATION PARAMETERS.

	Parameters
Number of users	100
Number of cells	7 (the 1st tier is considered)
Number of carriers	1024
Total Bandwidth	10 MHz
Orthogonality parameter	0.05

distance, for several different orthogonal parameters. It can be seen that E_b/N_0 rapidly drops near the cell boundary due to ICI, even if a smaller orthogonal parameter is used. However, the radio resources can be allocated to each layer as a function of visual weight, and the UEP algorithm can be conducted.
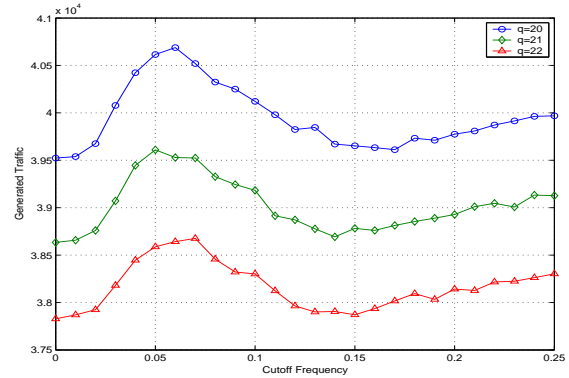
Fig. 8. The total traffic of the layered coding scheme as a function of cutoff frequency
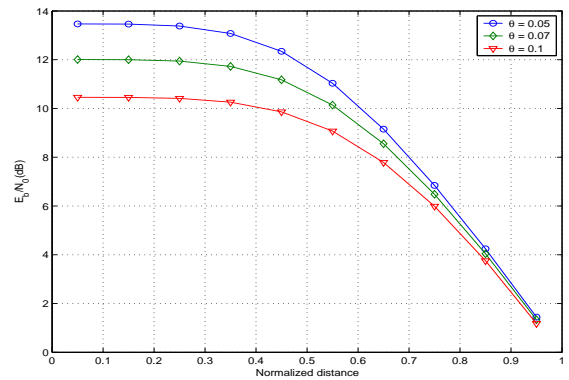
Fig. 9. E_b/N_0 as a function of normalized distance for orthogonal parameters
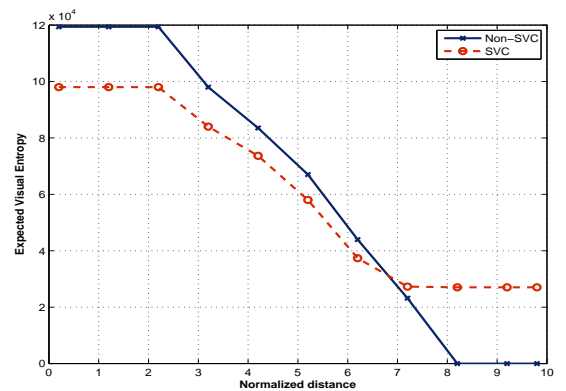
Fig. 10. The expected visual entropy as a function of normalized distance for the intra-frame

Figure 10 compares the delivered visual entropy between the conventional non-scalable and scalable video schemes as a function of normalized distance for the first intra-frame.
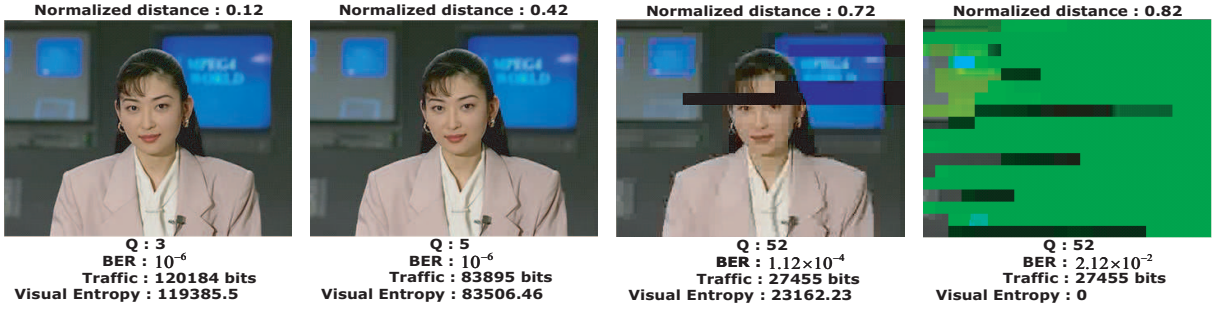
Fig. 11. Reconstructed video quality of the non-layered coding scheme
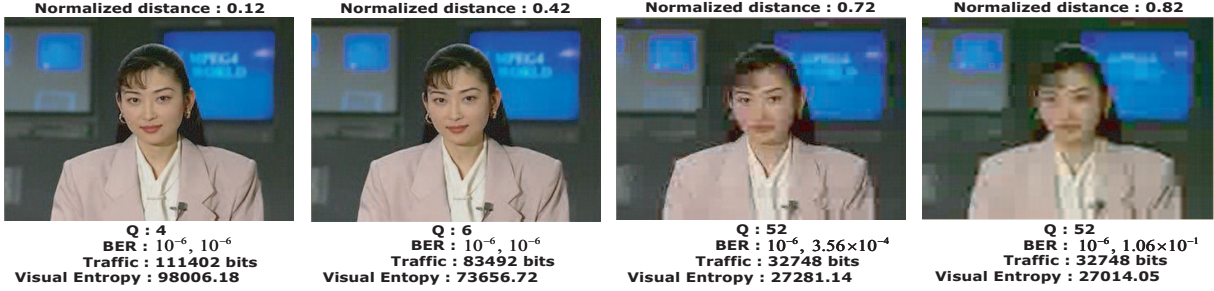
Fig. 12. Reconstructed video quality of the layered coding scheme

Using non-scalable video, more visual entropy is delivered relative to scalable video when the channel state is reliable. In the normalized distance range 0 to 0.62, the video bit stream is delivered to the user without any transmission errors. Therefore the difference in the visual entropy depends on the amount of coding redundancy.

However, if the channel becomes unreliable due to ICI as shown in Fig.9, a crossing point of the expected visual entropy occurs around a normalized distance of 0.7 as shown in Fig.10. At this distance the channel quality starts to rapidly drop, and so visually important low frequency information in a non-layered coding approach can be lost. At a normalized distance of 0.8, the visual entropy is nearly zero. At this distance, the amount of generated traffic is much higher than the link capacity even if a maximum QP is used. Thus, more visual information is lost due to the limited link budget. Conversely, in scalable video the throughput of the base layer can be preserved due to being preferentially guaranteed. Much higher throughput of visual entropy can be maintained at the cell boundary by using the optimal approach. In order to achieve the best performance, it is advisable to employ an adaptive coding scheme that depends on the channel status, by using non-scalable video for the reliable channel and vice versa.

In Fig. 11 and Fig. 12, the reconstructed picture quality is demonstrated as a function of normalized distance. The quality of the non-scalable video is improved by using a lower QP when the channel state is reliable. On the other hand, when the channel state become unreliable, the non-scalable video traffic can exceed the channel link capacity, and severe quality degradation can be observed at normalized distances of 0.82. In SVC, the channel throughput of the base layer can be maintained even at the cell boundary, owing to the reduced traffic volume relative to the enhancement layer. The reconstructed picture is distorted (blurred) by delivering the bitstream of the base layer.

VII. CONCLUSION

We have developed a cross-layer optimization framework that operates between the application and MAC/PHY layers. On the source side we utilized the SVC coder, which is suitable for deriving perceptual weights. The visual entropy is defined by applying the perceptual weights to the empirical rate model of the SVC. On the channel side, the ratio E_b/N_o of the OFDM-based system is modeled as a function of normalized distance, in terms of the number of sub-carriers and the user bit rate. By deploying the expected visual entropy as an objective function, an optimization problem can be formulated. However, since the optimization problem is computationally intractable, sub-optimal values of the expected visual entropy can be found by using a greedy algorithm. In the simulations, it was observed that the performance of non-scalable video is better than that of scalable video within the inner region. In the outer region, however, non-scalable video is almost destroyed by ICI, whereas scalable video provides at least an acceptable quality. The criteria that makes it possible to determine which coding method is more effective for a given channel status is therefore quite useful for achieving seamless real-time video service.

REFERENCES

[1] H. Son and S. Lee, "Bandwidth and region division for broadband multi-cell networks," *IEEE Comm. Letter.*, vol. 10, pp. 360-362, May 2006.
[2] Samsung, "Flexible fractional frequency reuse approach," 3GPP, TSG RAN WG1, R1-051341, Seoul, Korea, November, 2005.
[3] H. Jiang, W. Zhuang and X. Shen, "A cross-layer design for resource allocation in 3G wireless networks and beyond," *IEEE Commun. Mag*, vol. 43, pp. 120-126, Dec. 2005.

[4] H. Schwarz, D. Marpe and T. Wiegnd, "Overview of the scalable video coding extention of the H.264/AVC standard," *IEEE Trans. Circuit Syst. Video Technol,* vol. 17, no. 9, pp. 1103-1120, Sept. 2007.

[5] M. Wien, H. Schwarz and T. Oelbaum, "Performance analysis of SVC," *IEEE Trans. Circuit Syst. Video Technol,* vol. 17, no. 9, pp. 1194-1203, Sept. 2007.

[6] T. Schierl, T. Stockhammer and T. Wiegand, "Mobile video transmission using scalable video coding," *IEEE Trans. Circuit Syst. Video Technol,* vol. 17, no. 9, pp. 1204-1217, Sept. 2007.

[7] D. Wu, Y. T. Hou and Y.-Q. Zhang, "Scalable video coding and transport over broad-band wireless networks," *Proc. IEEE,* vol. 89, pp. 6-20, Jan. 2001.

[8] N. Conci, G. B. Scorza and C. Sacchi, "A cross-layer approach for efficient MPEG-4 video streaming using multicarrier spread-spectrum transmission and unequal error protection ," *IEEE Int. Conf. Image Processing,* Genova, vol. 1, pp. 11-14, Sept. 2005.

[9] S. Lee, M. S. Pattichis, and A. C. Bovik, "Foveated video quality assessment," *IEEE Trans. Multimedia,* vol. 3, pp. 129-132 2001.

[10] B. Griod, "What's wrong with mean-squire error," *Digital Images and Human Vision,* A. B. Watson, Ed. Cambridge, MA: MIT Press, pp. 207-220, 1993.

[11] H. Son and S. Lee, "Forward link capacity analysis for MC-CDMA," *IEICE Trans. COMMUN.,* vol. E88-B, pp. 4094-4096, June 2005.

[12] S. Lee, M.S. Pattichis and A.C. Bovik, "Foveated video compression with optimal rate control," *IEEE Trans. Image Processing,* vol. 10, pp.977-992, Jul. 2001.

[13] S. Wenger, Y.-K. Wang, and T. Schierl, "Transport and signaling of SVC in IP networks," *IEEE Trans. Circuits Syst. Video Technol.,* vol. 17, no. 9, pp. 1164-1173, Sep. 2007.

[14] N. Tizon and B. P. Popescu "Scalable and media aware adaptive video streaming over wireless networks," *EURASIP Journal on Advances in Signal Processing,* vol. 2008, artical ID 218046, pp. 1-11, May 2008.

[15] H.-M. Hang and J.-J. Chen, "Source model for transform video coder and its application.part I: fundamental theory," *IEEE Trans. Circuit Syst. Video Technol,* vol. 7, no. 2, pp. 197-211, Apr. 1997.

[16] Z. Wang and A.C. Bovik, "Embedded foveation iamge coding," *IEEE Trans. Image Processing,* vol. 10, no. 10, pp.1397-1410, Oct. 2001.

[17] S. Lee and A. C. Bovik, "Fast algorithms for foveated video processing," *IEEE Trans. Circuit Syst. Video Technol.,* vol. 13, pp. 149-162, February 2003.

[18] W. S. Geisler and J. S. Perry, "A real-time foveated multiresolution system for low-bandwidth video communication," *Proc. SPIE,* vol. 3299, 1998.

[19] B. Chitprasert and K. R. Rao, "Human visual weighted progressive image transmission, *IEEE Trans. Commun.,* vol. 38, pp. 1040.1044, July 1990.

[20] John G. Proakis, "Digital Communications," *4th edition,* Mc Graw Hill 1995.

[21] Z. G. Li, W. Gao, F. Pan, S. W. Ma, K. P. Lim, G. N. Feng, X. Lin, S. Rahardja, H. Q. Lu and Y. Lu, "Adaptive Rate Control for H.264," *Journal of Visual Communication and Image Representation*, vol. 17, no. 2, pp. 376-406, Apr, 2006

[22] J. Reichel, H. Schwarz, M. Wien, eds., "Joint scalable video model 11 (JSVM 11)," *Joint Video Team,* doc. JVT-X202, Geneva, Switzerland, July 2007.

Jincheol Park was born in Korea in 1982. He received his B.S. degree in Information and Electronic Engineering from Soongsil University, Seoul, Korea in 2006. He received his M.S. degree in Electrical and Electronic Engineering from Yonsei University, Seoul, Korea in 2008. He is currently pursuing the the Ph. D. from 2008 in Wireless Network Laboratory from Yonsei University, Seoul, Korea. His research interests include wireless multimedia communications and video quality assessment.

Hyungkeuk Lee was born in Korea in 1977. He received his B.S. degree and the M.S. degree in Electrical and Electronic Engineering from Yonsei University, Seoul, Korea in 2005 and 2006, respectively. He is currently working toward the Ph. D. from 2006. In 2008, he was a Visiting Researcher in the Laboratory for Image and Video Engineering (LIVE) of Prof. Alan C. Bovik at The University of Texas at Austin. His research interests include wireless resource allocation based on economics, video coding and cross-layer optimization.

Sanghoon Lee was born in Korea in 1966. He received his B.S. in E.E. from Yonsei University in 1989 and his M.S. in E.E. from Korea Advanced Institute of Science and Technology(KAIST) in 1991. From 1991 to 1996, he worked for Korea Telecom. He received his Ph.D. in E.E. from the University of Texas at Austin in 2000. In June - Aug. 1999, he worked for Bell-Lab., Lucent Technologies on wireless multimedia communications. From Feb. 2000 to Dec. 2002, he worked on developing real-time embedded software and communication protocols for 3G wireless networks, Lucent Technologies. In March 2003, he joined the faculty of the Department of Electrical & Electronics Engineering, Yonsei University, Seoul, Korea, where he is an Associate Professor. Hi is JOURNAL of COMMUNICATIONS and NETWORKS (JCN) associate editor. He is interested in video quality assessment, wireless network, sensor network and multimedia communications.

Alan Conrad Bovik (S′80_M′81_SM′89_F′96) received the B.S., M.S., and Ph.D. degrees in electrical and computer engineering from the University of Illinois at Urbana-Champaign, Urbana, in 1980, 1982, and 1984, respectively. He is currently the Curry/Cullen Trust Endowed Professor at The University of Texas at Austin, where he is the Director of the Laboratory for Image and Video Engineering (LIVE) in the Center for Perceptual Systems. His research interests include image and video processing, computational vision, digital microscopy, and modeling of biological visual perception. He has published over 450 technical articles in these areas and holds two U.S. patents. He is also the author of The Handbook of Image and Video Processing (Elsevier, 05, 2nd ed.) and Modern Image Quality Assessment (Morgan & Claypool, 2006). Dr. Bovik has received a number of major awards from the IEEE Signal Processing Society, including: the Education Award (2007); the Technical Achievement Award (2005); the Distinguished Lecturer Award (2000); and the Meritorious Service Award (1998). He is also a recipient of the Distinguished Alumni Award from the University of Illinois at Urbana-Champaign (2008), the IEEE Third Millennium Medal (2000), and two journal paper awards from the International Pattern Recognition Society (1988 and 1993). He is a Fellow of the Optical Society of America the Society of Photo-Optical and Instrumentation Engineers. He has been involved in numerous professional society activities, including: Board of Governors, IEEE Signal Processing Society, 19961998; Editor-in-Chief, IEEE TRANSACTIONS ON IMAGE PROCESSING, 19962002; Editorial Board, PROCEEDINGS OF THE IEEE, 19982004; Series Editor for Image, Video, and Multimedia Processing, Morgan and Claypool Publishing Company, 2003_present; and Founding General Chairman, First IEEE International Conference on Image Processing, Austin, TX, November 1994. He is a registered Professional Engineer in the State of Texas and is a frequent consultant to legal, industrial, and academic institutions.